A sequential mechanism for clathrin cage disassembly by 70-kDa heat-shock cognate protein (Hsc70) and auxilin

Alice Rothnie[a], Anthony R. Clarke[b], Petr Kuzmic[c], Angus Cameron[b], and Corinne J. Smith[a,1]

[a]School of Life Sciences, Warwick University, Gibbet Hill Road, Coventry CV4 7AL, United Kingdom; [b]Department of Biochemistry, University of Bristol, Bristol BS8 1TD, United Kingdom; [c]BioKin, Ltd., 15 Main Street Suite 232, Watertown, MA 02472

An essential stage in endocytic coated vesicle recycling is the dissociation of clathrin from the vesicle coat by the molecular chaperone, 70-kDa heat-shock cognate protein (Hsc70), and the J-domain-containing protein, auxilin, in an ATP-dependent process. We present a detailed mechanistic analysis of clathrin disassembly catalyzed by Hsc70 and auxilin, using loss of perpendicular light scattering to monitor the process. We report that a single auxilin per clathrin triskelion is required for maximal rate of disassembly, that ATP is hydrolyzed at the same rate that disassembly occurs, and that three ATP molecules are hydrolyzed per clathrin triskelion released. Stopped-flow measurements revealed a lag phase in which the scattering intensity increased owing to association of Hsc70 with clathrin cages followed by serial rounds of ATP hydrolysis prior to triskelion removal. Global fit of stopped-flow data to several physically plausible mechanisms showed the best fit to a model in which sequential hydrolysis of three separate ATP molecules is required for the eventual release of a triskelion from the clathrin–auxilin cage.

clathrin-mediated endocytosis | kinetic mechanism | macromolecular assemblies | vesicle uncoating | mathematical model

Endocytosis is at the center of a hub of cellular processes that include nutrient uptake, receptor down-regulation, synaptic vesicle recycling, signaling, and developmental processes (1). During clathrin-mediated endocytosis, the cell membrane invaginates to form a bud in which receptors with specific cargo accumulate. The bud encloses the cargo and forms a vesicle that becomes detached from the membrane, moving on to fuse with its target compartment. This process is directed by a network of proteins that dictate how and when the bud forms, which receptors are included in the vesicle, and which ensure that the vesicle is completed and detached from the membrane. Some of these proteins, including clathrin and AP2, form a coat around the vesicle while it is forming and help to select the cargo that is enclosed (2–5). After detachment, the protein coat is quickly removed, and the vesicle goes on to fuse with its target membrane. This process of uncoating is essential and primarily involves the molecular chaperone, 70-kDa heat-shock cognate protein (Hsc70), and its DnaJ cofactor, auxilin/cyclin-G-associated kinase. As well as their role in uncoating, Hsc70 and auxilin interact with other proteins, indicating their possible involvement in related processes such as vesicle movement and vesicle formation (6).

Clathrin can be purified and assembled, in vitro, into polyhedral cages that resemble the clathrin coats observed in cells. Monitoring of cage disassembly in vitro has allowed the disassembly of clathrin cages into individual clathrin triskelions by Hsc70 and auxilin to be well-characterized in biochemical terms. Through the work of a number of different groups, the essential domains of auxilin and Hsc70 required for clathrin disassembly have been established (7, 8), affinities of Hsc70 for auxilin (9, 10) and nucleotides (11, 12) have been determined, and the stoichiometric relationships between clathrin, Hsc70 and auxilin during

disassembly have been investigated. It has been proposed that three molecules of Hsc70 are involved in removing one triskelion from a coated vesicle (13). This is supported by electron microscopy and gel filtration data that showed three Hsc70 molecules bound to the released triskelia (14, 15) and by demonstration of maximal binding to cages of three Hsc70s per triskelion (16). However, interestingly, Xing et al. (17) report a stoichiometry of about one Hsc70 molecule per threefold clathrin vertex in their recent cryoelectron microscopy study of Hsc70 bound to clathrin cages. Maximal binding of auxilin to clathrin cages has been shown to occur at a ratio of three molecules per triskelion (7, 18), yet substoichiometric amounts of auxilin can support complete cage disassembly (19, 20). Intriguingly, only a single auxilin per triskelion is required for maximal stimulation of ATP hydrolysis by Hsc70 (9) or maximal binding of Hsc70 to clathrin (16).

In light of these data, a model for disassembly was proposed by Ungewickell et al. (16) that depicts a single auxilin molecule binding per clathrin triskelion, each of which recruits three molecules of Hsc70, and upon hydrolysis of ATP, conformational changes distort the triskelia and cage disassembly occurs. Given that auxilin and Hsc70 are known to interact at a 1:1 stoichiometry in solution (7, 10), this model raises an important question: By what mechanism can a single auxilin recruit three Hsc70 molecules?

In this paper, we address this problem via kinetic analysis of cage disassembly based on light-scattering measurements. It was recently demonstrated that dynamic light scattering can be used effectively to monitor clathrin cage disassembly (21, 22), thus providing better time resolution than previous studies that were predominantly based on centrifugation and densitometry of SDS-PAGE (19, 20). We have further increased the time resolution by which disassembly kinetics can be measured, by monitoring simple perpendicular light scattering using stopped-flow methods to capture events on the milliseconds-to-seconds timescale. This has allowed us to observe a previously unseen stage in the recruitment of Hsc70 to clathrin cages. We have also determined the amount of phosphate released per triskelion while cage disassembly is taking place, and, in addition, we show that only a single auxilin per triskelion is required for the maximum rate of clathrin cage disassembly by Hsc70, thus demonstrating the functional significance of the stoichiometry of the interaction of auxilin with clathrin and Hsc70 shown previously. Statistical analysis of our data according to five physically plausible mechanistic models

BIOCHEMISTRY

revealed that a three-step sequential mechanism fitted the data most accurately. Based on these results, we propose a sequential recruitment model for the action of Hsc70 on clathrin cages, which explains both our observations and previously published data.

Results

The Light-Scattering Assay.
In these measurements, perpendicular light scattering is used to monitor the real-time disassembly of clathrin cages by Hsc70, ATP, and auxilin ($GSTaux_{401-910}$). Upon addition of Hsc70 and ATP to clathrin cages with auxilin bound, the scattering signal decreases rapidly as the cages are disassembled into triskelia (Fig. 1A). We clarified the meaning of this signal by imaging the disassembly process using transmission electron microscopy. Samples were taken at specific time points during disassembly reactions and negatively stained EM grids prepared. For each time point, multiple images were obtained and the number of cages per image counted. These assays were conducted under conditions where the Hsc70 concentration was low so that sufficient intermediate time points could be captured using negative staining. Fig. 1 C–E shows representative images from three grids prepared at different time points during a single disassembly reaction. The average results of the EM cage-counting assay for three different concentrations of Hsc70 in Fig. 1B show an excellent correlation between the decay in cage numbers counted and the decay in light scattering.

The Dependence of Cage Disassembly on Hsc70 and Auxilin Concentrations.
We then used the light-scattering assay to monitor the effect of varying the concentrations of auxilin and Hsc70 on the time-course of cage disassembly. Representative data for these measurements are shown in Fig. 2 A and D. At fixed concentrations of clathrin (0.09 μM triskelia) and auxilin (0.3 μM), increasing the concentration of Hsc70 leads to an increase in the rate at which disassembly occurs (Fig. 2A). Using the time taken to disassemble half of the clathrin cages, $t_{1/2}$, as a measurement for the rate of disassembly (Fig. 2B) it can be seen that an excess of Hsc70 is required to reach the maximal rate of disassembly.

The amplitude plot shown in Fig. 2C demonstrates that at low concentrations of Hsc70, the disassembly curves do not decay to zero; i.e., disassembly of clathrin cages under conditions of limiting Hsc70 is incomplete. This result suggests that the Hsc70 is not recycled and that, after cage disassembly driven by ATP hydrolysis, the resultant $Hsc70 : ADP(P_i)$ species remains tightly bound to the dissociated triskelia. To support this conclusion, subsequent addition of Hsc70 allows disassembly to proceed to completion (Fig. S1).

When the dependence of disassembly rate on auxilin concentration is analyzed (Fig. 2E), we observe a linear relationship between rate and auxilin concentration until a distinct break point is reached. This result shows there is a very tight interaction between auxilin and the assembled clathrin cages. This functional assay is relevant to the stoichiometry that governs the rate of the uncoating process. The maximum rate is achieved at a stoichiometry of 1 mol of auxilin to 1 mol of clathrin triskelion. It is also evident that complete disassembly occurs even at very low, substoichiometric concentrations of auxilin (Fig. 2F). This suggests that auxilin is recycled during the disassembly process.

The Role of Nucleotide Hydrolysis in Clathrin Cage Disassembly.
The hydrolysis of ATP is an obligatory step in clathrin cage disassembly and disassembly does not occur in the presence of nonhydrolyzable ATP analogues (Fig. S2). The rate of ATP hydrolysis by Hsc70 alone is very slow ($k = 0.0011 \pm 0.0002$ s^{-1}, Table S1), and it has been previously reported that interaction with both auxilin and clathrin can stimulate hydrolysis (7, 9, 10), as we also find (Table S1). However, these previous measurements have been carried out at pH 6, under conditions where disassembly is not observed. In order to understand how ATP hydrolysis might be coupled to clathrin cage disassembly, we measured the ATP hydrolysis that occurred during a clathrin cage disassembly reaction when the concentration of Hsc70 is in excess. Fig. 3 shows the amount of P_i produced under disassembly conditions (i.e., when the system is functionally coupled). The curve shows a rapid initial phase followed by a slow steady-state rate. The initial nonlinear region corresponds to the activity during cage disassembly,
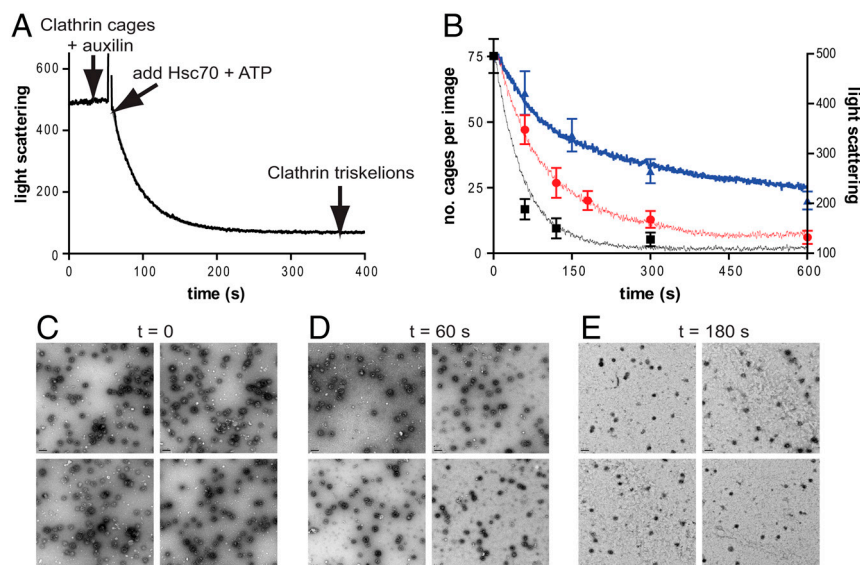

Fig. 1. A real-time in vitro assay for clathrin cage disassembly and correlation with electron microscopy images of clathrin cages. (A) Representative trace of the right-angle light-scattering assay for clathrin cage disassembly. Clathrin cages (0.09 μM triskelia) were premixed with 0.1 μM auxilin, and after 60 s, cage disassembly was initiated by addition of 1 μM Hsc70 and 500 μM ATP. (B) Average results for three different disassembly assays monitored both by light scattering as in A and compared with electron microscopy images as in C–E. The single points represent the average number of cages counted per image, initiated with 0.1 μM (triangles), 0.2 μM (circles), or 0.5 μM (squares) Hsc70. Data are mean ± SD. The single lines represent the light-scattering results obtained under the same conditions. (C–E) Representative transmission electron micrographs of negatively stained grids prepared at 0, 60, and 180 s during a disassembly assay containing clathrin cages (0.09 μM triskelia), 0.1 μM auxilin, 500 μM ATP, and initiated with 0.2 μM Hsc70. The scale bar in the bottom left-hand corner of each image represents 0.2 μm.
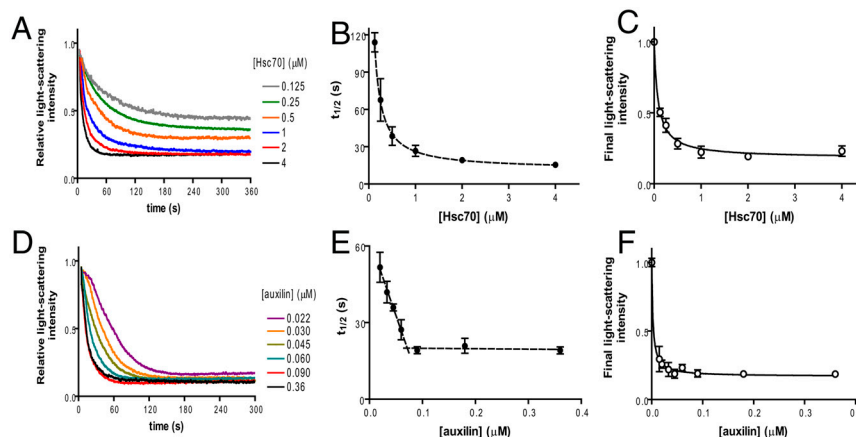
Fig. 2. The effect of [Hsc70] or [auxilin] on clathrin cage disassembly. (*A*) Representative light-scattering curves containing clathrin cages (0.09 μM triskelia), auxilin (0.3 μM), and ATP (500 μM) with disassembly initiated by various concentrations of Hsc70 (0.15–4 μM). (*D*) Representative disassembly curves with clathrin cages (0.09 μM triskelia) premixed with varying [auxilin] (0.022–0.36 μM) and 500 μM ATP, and initiated by addition of 2 μM Hsc70. (*B* and *E*) Symbol $t_{1/2}$ on the vertical axis denotes the average time taken for disassembly of 50% of clathrin cages obtained from raw data traces as in *A* and *D*, respectively. Data points and error bars, respectively, are mean ± standard error from replicated measurements ($n \geq 4$). (*C* and *F*) Average amplitude (total amount of disassembly) at the end of each assay from curves obtained as in *A* and *D*, respectively. Data points and error bars, respectively, are mean ± standard error from replicated measurements ($n \geq 4$). The smooth curves in panels *B*, *C*, and *F* represent a fit to the hyperbolic saturation function (Eq. S1), which serves as an empirical description of the data.

and the rate at which ATP is hydrolyzed during this time is comparable to the rate of clathrin disassembly ($t_{1/2} \approx 15$ s). The later, linear steady-state rate is simply the basal activity of Hsc70 plus any stimulation from the low concentration of auxilin present, and this rate agrees well with our steady-state data (Table S1). Interestingly, these data show that approximately 1 mol of ATP is hydrolyzed during the disassembly of 1 mol of clathrin heavy chain, or 3 mol of ATP per clathrin triskelion released. This stoichiometry suggests that either three Hsc70s bind to a triskelion and each hydrolyzes a single ATP, or a single Hsc70 binds per triskelion and hydrolyzes three ATPs. If three Hsc70s bind, they might bind clathrin and each hydrolyze one ATP at the same time or in series. If the process happened in series, ATP ligands would be hydrolyzed one after the other with disassembly only occurring after the final hydrolysis. If a single Hsc70 is required to turn over three ATPs consecutively, or if three Hsc70s work in series, this would result in a lag phase early in the disassembly process while the first two rounds of hydrolysis occurred.

Early Events in Clathrin Cage Disassembly. To study the early events in disassembly and ascertain if there is a lag phase, we performed the scattering assay in a stopped-flow fluorimeter, which allowed us to decrease the dead time from 4–6 s in the standard fluorimeter to less than 10 ms. Results from the stopped-flow experi-

ments are shown in Fig. 4, and demonstrate that there is indeed a lag phase before disassembly begins. Strikingly, in addition to the lag phase, there is a significant increase in the scattering signal before the disassembly process begins. Both the rate and amplitude of this initial increase in scattering are dependent on the concentration of Hsc70. Factors that give rise to changes in light-scattering signal include changes in molecular weight or in radius of gyration. Because we observe a process that depends upon Hsc70 concentration and yet is not indicative of a simple binding interaction, we propose that this increase in scatter represents Hsc70 recruitment to the cage complex, accompanied by a conformational change in the complex that alters its radius of gyration. We interpret the lag phase as being due to the first two rounds of ATP hydrolysis per triskelion by Hsc70, after which, upon the third round of ATP hydrolysis, the triskelion dissociates and the scattering signal starts to decrease.

In order to test our conclusions, we fitted five alternative kinetic mechanisms (Schemes S3–S7) to the stopped-flow data. The fit of the simplest plausible mechanism consistent with the data (Scheme 1) is shown in Fig. 4. The light-scattering data agree well with a mechanism in which an initial binding event is accompanied by an increase in molar scattering followed by two more binding events and a loss of scattering on disassembly
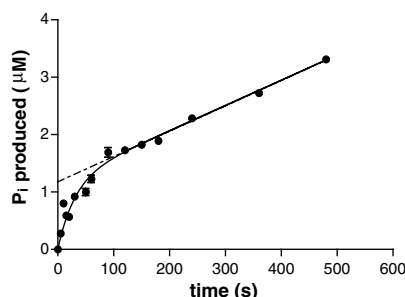
Fig. 3. The hydrolysis of ATP during clathrin cage disassembly. The amount of P_i produced from ATP hydrolysis by Hsc70 during clathrin cage disassembly was monitored. Clathrin (0.33 μM triskelia), 0.35 μM auxilin, and 8 μM Hsc70 were mixed together. The reaction was initiated by addition of ATP (50 μM), and at specific time points samples were removed, quenched, and assayed for P_i content with malachite green solution. The data are fitted to a single exponential superimposed on a linear function (Eq. S2).
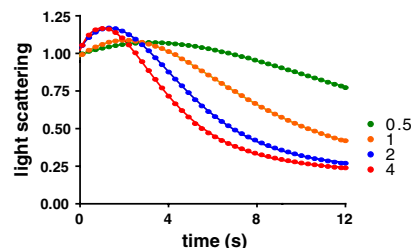
Fig. 4. Stopped-flow measurements of light scattering to examine the early stages of clathrin cage disassembly. Clathrin cages (0.09 μM triskelia) premixed with 0.1 μM auxilin were mixed with Hsc70 (concentrations in μM shown on graph) and 500 μM ATP, and perpendicular light scattering was measured using stopped-flow techniques. The closely spaced raw data was reduced to a frequency of 3.3 s^{-1} (closed circles) and fitted (dashed lines) to a system of first-order ordinary differential equations corresponding to the reaction mechanism shown in Scheme 1, using the software DYNAFIT (29, 30). Data corresponding to 0 and 0.25 μM Hsc70 were omitted from the fit because of their low information content, as was data collected after 12 s.

$$C \xrightarrow[\text{+T}]{k_a} CT \xrightarrow{k_r} CD \xrightarrow[\text{+T}]{k_a} CDT \xrightarrow{k_r} CDD \xrightarrow[\text{+T}]{k_a} CDDT \xrightarrow{k_r} CDDD \xrightarrow{k_d} P$$

C = clathrin•auxilin
T = Hsc70•ATP
D = Hsc70•ADP
P = *products*
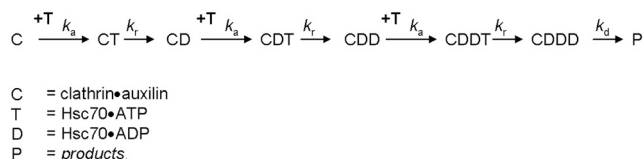
Scheme 1. The three-step sequential mechanism for clathrin cage disassembly that fitted the kinetic data most accurately when five alternate kinetic mechanisms were tested (Schemes S3–S7). Each step consists of an association event between clathrin.auxilin (C) and Hsc70.ATP (T) with rate constant k_a, followed by hydrolysis of ATP to ADP with rate constant k_r. Once the three steps have taken place, the clathrin.auxilin cage disassembles with rate constant k_d.

(Scheme 1 and Table 1). Three unique rate constants, k_a, k_r and k_d, are required to describe the data taking the values of $0.69~\mu M^{-1}~s^{-1}$, $6.5~s^{-1}$, and $0.38~s^{-1}$, respectively. In Scheme 1, the three unique rate constants appear altogether in seven separate steps. The first six steps are pairs of consecutive association-hydrolysis reactions, each characterized by rate constants k_a and k_r, respectively. The final step is the cage disassembly itself, characterized by the rate constant k_d. Although we initially allowed every binding and hydrolysis step to take different values, it became apparent that this offered no statistical advantage over a simpler scheme where two rate constants described the binding of Hsc70 and turnover of ATP (see *SI Text*). Reducing the number of binding/hydrolysis steps from three to two (Scheme S5) resulted in a 20% increase in the residual sum of the squares and was not favored by the Akaike information criterion (23), which properly accounts for differing number of adjustable parameters used in the models (Table S2). Variations on the three-step model depicted in Scheme 1 were tested, but we were unable to confidently distinguish between "semiconcerted" models that allowed binding of two Hsc70 molecules before the first hydrolysis step and the fully sequential Scheme 1. A "fully concerted" scheme, Scheme S6, where binding of three Hsc70s takes place before hydrolysis was not favored, further supporting a mechanism involving a stepwise process of Hsc70 binding and ATP hydrolysis. The fact that three microscopic rate constants, k_a, k_r, and k_d, are required to describe the data would suggest that the clathrin disassembly progress curves should be fitted well by a triple exponential model, and this is indeed the case (Fig. S3).

Discussion

Using a simple perpendicular light-scattering assay we have measured the in vitro disassembly of clathrin cages by Hsc70 and auxilin, which occurs rapidly with a $t_{1/2}$ of approximately 10 s. This is comparable to recent results from experiments that used dynamic light scattering to monitor clathrin cage disassembly (21, 22) but faster than earlier centrifugation-based studies that had $t_{1/2}$ values ranging from 2–10 min (19, 20, 24) but that also contained adaptor proteins such as AP180 or AP2, which are known to stabilize the cages and may consequently have slowed down disassembly. In this study, we have increased the time resolution beyond that of dynamic light scattering by monitoring perpendicular light scattering, and analysis of these data has allowed us to isolate and describe individual steps in the chaperone-mediated disassembly of cages that hitherto have remained invisible.

The veracity of the scattering signal in representing the true disassembly reaction was established by correlating the cage count with the scattering intensity. This required using time-resolved sampling with electron microscopy and comparing this with the scattering intensities. Our data show an excellent correlation and demonstrate that the decrease in scattering signal is proportional to the number of cages throughout the progress of the reaction.

The data we have collected on the concentration dependence of disassembly kinetics (Fig. 2) reveal that, whereas an excess of Hsc70 is required to achieve the maximal rate of uncoating, a ratio of only one auxilin molecule per triskelion is required to achieve this. Our phosphate release experiments (Fig. 3) show that three ATP molecules must be hydrolyzed for every triskelion released. These results raised two important questions. (*i*) What features of the mechanism cause triskelion release after hydrolysis of three ATP molecules? (*ii*) How can a single auxilin molecule coordinate the release of one triskelion?

Here, we propose a model for the mechanism by which Hsc70 and auxilin act to disassemble clathrin cages based on analysis of our stopped-flow light-scattering data, which answers these questions and defines this mechanism more fully than has been previously possible. The model is illustrated in Fig. 5. Firstly, auxilin binds tightly to the clathrin cages, at a ratio of one auxilin per triskelion to achieve the optimum rate of disassembly. The Hsc70:ATP complex then binds to the clathrin–auxilin cage, initially at a ratio of one Hsc70 per triskelion. The interaction of this Hsc70 with the J domain of auxilin stimulates the hydrolysis of ATP, causing a conformational change in the Hsc70 in which the Hsc70:ADP complex is firmly attached to its binding site on clathrin. Following this, a second Hsc70:ATP is recruited to the clathrin:auxilin complex, a further ATP is hydrolyzed, and the second Hsc70 is attached. Finally, the third Hsc70:ATP is recruited to the clathrin–auxilin complex, and upon ATP hydro-
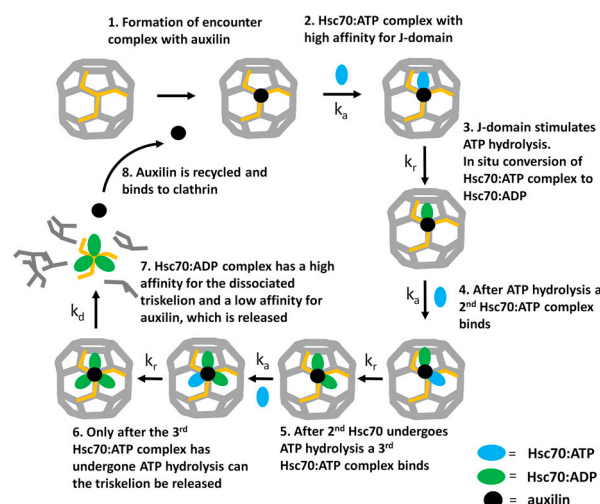
Fig. 5. An illustration of the serial Hsc70 binding and ATP hydrolysis model for the disassembly of clathrin cages highlighting the sequence of events on a single triskelion. 1: Auxilin has a high affinity for triskelion legs forming part of a clathrin cage and binds at a stoichiometry of one per triskelion. 2: An Hsc70:ATP complex binds to the clathrin:auxilin complex. 3: The interaction between auxilin's J domain and Hsc70 stimulates ATP hydrolysis and induces a conformational change in Hsc70, increasing its affinity for clathrin. 4: Auxilin repositions, and a second Hsc70:ATP is recruited to the clathrin:auxilin complex. 5: The second Hsc70 interacts with auxilin's J domain, ATP is hydrolyzed, and the resulting Hsc70:ADP complex binds tightly to clathrin. Following hydrolysis, the auxilin again repositions, and a third Hsc70:ATP binds to the clathrin:auxilin complex. 6: Hydrolysis of the third ATP results in a weak interaction between the triskelion(Hsc70:ADP)$_3$ complex and the cage. The rate-limiting step is the disassembly of triskelia leading to cage collapse. 7: The Hsc70:ADP complex has a high affinity for the released triskelia and remains bound, whereas the affinity of triskelia(Hsc70:ADP)$_3$ for auxilin is low; the previously bound auxilin is free now to rebind the cage in a catalytic manner (8).

Table 1. Kinetic parameters for the reaction mechanism depicted in Scheme 1

Parameter	Best-fit value	99% confidence interval
k_a, $\mu M^{-1}~s^{-1}$	0.69	0.67–0.72
k_r, s^{-1}	6.5	5.3–8.4
k_d, s^{-1}	0.38	0.37–0.39

Rothnie et al.

lysis by this molecule the conformational strain imposed upon the clathrin by its interaction with Hsc70:ADP leads to a concerted dismantling of the cage into component triskelia. The three Hsc70:ADP molecules have a high affinity for the released triskelia and therefore remain tightly bound and are not recycled. In contrast, auxilin has a low affinity for the released triskelia and Hsc70-ADP and can therefore dissociate and be recycled.

Our suggestion that Hsc70-ADP remains tightly bound to the released triskelia comes from the amplitude data in Fig. 2C, which shows that disassembly does not proceed to completion when limiting concentrations of Hsc70:ATP are used. The reaction will, however, proceed further when additional Hsc70:ATP is added subsequently (Fig. S1). This agrees well with previous studies that have shown Hsc70 bound to the free triskelia (14, 15, 22) and supports the idea previously proposed that Hsc70 acts to chaperone the released clathrin triskelia back to the plasma membrane (25), preventing formation of empty cages within the cell. It should be noted that, in a similar previous study, Schuermann et al. (22) also observed a second, slower linear phase of disassembly following the initial fast exponential phase. We do not observe this second slower phase in our studies, but this may simply reflect small differences in assay conditions, which may affect the strength of the binding interaction between Hsc70:ADP and clathrin. It should also be noted that, in vivo, nucleotide exchange factors interact with Hsc70, and it is likely that in the presence of such a nucleotide exchange factor we would observe recycling of Hsc70.

The requirement of a single auxilin per triskelion to achieve the maximum rate of disassembly is clearly shown from the stoichiometric point in our results in Fig. 2E. Interestingly, it has previously been shown that one auxilin per triskelion gives maximal stimulation of Hsc70 ATPase activity (9) and that a single auxilin bound per triskelion supported maximal Hsc70 binding (16). Thus, a ratio of one auxilin per clathrin triskelion appears to be of critical functional significance in the disassembly reaction. This is not to say that more auxilin cannot bind to clathrin—several reports have shown that much more auxilin than this can bind to clathrin (7, 18, 26), and three auxilins per triskelion are seen in a high-resolution EM structure (18). However these "extra" auxilin molecules are not required for the disassembly process, as we have shown that only a single auxilin per triskelion is required for optimum disassembly rates.

The time-resolved ATPase reactions (Fig. 3) show that three ATPs are hydrolyzed per triskelion released, a value in agreement with published data obtained for clathrin associated with AP180 (19). There are three possible explanations for this. Firstly, that three Hsc70 molecules bind per triskelion and each hydrolyzes one ATP in parallel reactions. Secondly, that a single Hsc70 binds per triskelion and hydrolyzes three ATPs in series. Thirdly, that three Hsc70s bind and hydrolyze ATP in series.

The second explanation, that a single Hsc70 molecule hydrolyzes three ATPs, contradicts extensive previous evidence that three Hsc70 molecules per triskelion are employed in the disassembly reaction. Previous binding studies have shown a maximal binding of three Hsc70s per triskelion at equilibrium (16, 24), and, like in our study, this was shown to occur with only a single auxilin per triskelion. It has also been shown that approximately three molecules of Hsc70 dissociate one triskelion when coated vesicles rather than empty cages were used (6) and it has been found that, following disassembly, three Hsc70s are bound to each free triskelion (14, 15). Identification of the Hsc70 binding motif and the location of this within the cage structure suggest that Hsc70 can bind to three potential binding sites on flexible regions protruding down from the hub (27).

This leaves us with an unusual stoichiometric situation, in which a single auxilin recruits three Hsc70 molecules, as has been suggested in previous models (6, 16). The interaction between the J domain of auxilin and Hsc70 is required for disassembly (16),

but the binding of Hsc70 to auxilin occurs at a 1:1 ratio (Table S1) (7, 10), so how does a single auxilin interact with three Hsc70 molecules? Our proposal that three Hsc70s are recruited and hydrolyze ATP in series would enable a single auxilin to stimulate the ATP hydrolysis by each Hsc70 in turn. In this model, auxilin and Hsc70 still interact at a 1:1 ratio at any one time, with auxilin dissociating and moving from one Hsc70 to the next following ATP hydrolysis and attachment of Hsc70:ADP to clathrin. Such a model is also consistent with the well-documented mechanism of other Hsp70/J domain systems (28). The evidence for the requirement of a series of steps to occur prior to triskelion release is provided by our stopped-flow scattering data (Fig. 4), which show a significant lag time before disassembly occurs. We tested the fit of our data to five related kinetic mechanisms (SI Text), all of which appear physically plausible. These include concerted, semiconcerted, and sequential mechanisms. The mechanism that fits optimally is an uncooperative, sequential, three-step process in which each Hsc70:ATP binds to the clathrin:auxilin cage and hydrolyzes the nucleotide with the same kinetic characteristics.

Where multiple binding events are proposed, it is logical to expect there to be cooperativity between binding sites, where sequential binding of ligand becomes tighter as the sites are occupied. For example, one might envisage that after the first Hsc70 binding and ATP hydrolysis step the corresponding triskelion leg becomes separated from the cage, causing a conformational change that makes binding of the second Hsc70 more likely, and so on. A possibility of such cooperative uncoating is contained within the molecular mechanism in Scheme S3, in which all microscopic rate constants are allowed to attain unique numerical values. However, this mechanism offered no statistical advantage over an otherwise identical model in which all three rate constants (either for Hsc70-ATP binding or for subsequent hydrolysis) kept the same value. We must therefore conclude that although cooperativity might in principle be present, it is weak to the point of being undetectable by our experimental method.

A recent cryo-EM structure (17) shows only around one Hsc70 bound per triskelion. In light of our model, this structure may represent an intermediate trapped in the first stage of this cycle at pH6, when only the first of the three Hsc70s has been recruited. The mechanism we propose also explains why three Hsc70s have been observed on released triskelions. Our proposed sequential mechanism is thus the simplest explanation that is consistent with both our results and previously published data.

Materials and Methods

Protein Expression and Purification. Full-length Hsc70 was expressed in Sf9 cells by infection with baculovirus and subsequently purified from the soluble cell lysate by a three-step chromatographic process comprising hydroxyapatite, ATP-agarose, and gel filtration. Residues 401–910 of bovine auxilin were expressed as a GST-fusion protein in Escherichia coli BL21 cells. GST-auxilin$_{401-910}$ was purified using a glutathione (GSH)-sepharose affinity column and is referred to elsewhere in this work as auxilin. The GST tag could optionally be cleaved off by incubation with thrombin and the GST removed by binding to GSH-sepharose beads. However, we observed no differences in the rates of clathrin disassembly and optimal stoichiometry with this cleaved auxilin compared to the GST-tagged version (Fig. S4). This is consistent with previous studies on the mechanism of auxilin function, which report no effect as a result of the presence of the GST tag (7, 8). Clathrin was purified from clathrin-coated vesicles that were extracted from pig brain by differential centrifugation and gel filtration. Clathrin cages were formed in vitro by dialyzing concentrated pure clathrin into buffer 7 [100 mM MES pH6.5, 15 mM MgCl$_2$, 0.2 mM EGTA, 0.02% (wt/vol) sodium azide], and harvested by centrifugation (135,000 × g, 20 min, 4 °C). For complete details on all these expression and purification procedures, see SI Text.

Light-Scattering Assays. Perpendicular light scattering was monitored using an LS50 fluorimeter (Perkin Elmer), at a wavelength of 390 nm (excitation and emission) and temperature of 25 °C. Unless otherwise stated in the figure legends, clathrin cages (0.09 μM triskelia), auxilin (0.015–0.36 μM), and ATP (500 μM) were premixed in a 60 μL total volume in buffer 2 (40 mM Hepes pH7, 75 mM KCl, 4.5 mM Mg acetate), and disassembly was initiated by

addition of 6 μL Hsc70 (0.8–40 μM). Light scattering was monitored every 0.25 s for up to 3,000 s. Control experiments were carried out to ensure that the scattering signal obtained from both clathrin cages and disassembled clathrin triskelia were linearly dependent on the clathrin concentration (Fig. S5). It was also determined that the interaction between Hsc70 and ATP is very rapid and that it was not necessary to premix Hsc70 with ATP as is typical in the literature (Fig. S6, SI Text, and Table S3). The time taken for disassembly of half of the clathrin cages was obtained from the raw data traces as the time taken for the light-scattering signal to decrease below 0.55. The amplitude of cage disassembly was obtained from the scattering signal remaining after 300 s. Increasing the time beyond this made no significant difference to the level of the scattering signal.

Stopped-flow perpendicular light scattering was measured using a BioLogic MOS450 stopped-flow fluorimeter. Unless otherwise stated in the figure legends, syringe 1 contained clathrin (0.17 μM triskelia) and auxilin (0.025–1 μM), and syringe 2 contained Hsc70 (0.5–8 μM) plus ATP (1 mM), all in buffer 2. These two solutions were rapidly mixed in the stopped-flow at a 1:1 ratio. Light scattering was monitored every 2 ms for up to 60 s. The excitation wavelength was 365 nm.

Electron Microscopy. Clathrin cages (0.09 μM triskelia) were premixed with auxilin (0.1 μM) and ATP (500 μM) in buffer 2, and cage disassembly was initiated by addition of Hsc70 (final concentrations of 0.1, 0.2, or 0.5 μM). At specific time points (0–15 min), samples were removed and negative-stain EM grids prepared immediately. Grids were imaged using a Jeol 2011 transmission electron microscope with LaB6 filament. Multiple images (10–15) were obtained for each grid, each from a different grid section, at a magnification of 10,000×. The number of cages per image were counted and averaged. In counting cages, we made no specific judgment as to whether a cage was complete or partial but simply counted all objects that had elements of polyhedral cage structure characteristic of clathrin assemblies.

ATPase Assay During Cage Disassembly. To measure the ATP hydrolysis during clathrin cage disassembly, P_i production was measured using the malachite green assay as previously described. Briefly, clathrin cages (0.33 μM triskelia) were mixed with auxilin (0.35 μM) and Hsc70 (8 μM) in buffer 2 at 25 °C. The reaction was initiated by addition of ATP (50 μM). At specific time points (5–480 s) samples were removed and mixed immediately with an equal volume of malachite green solution (0.3 mM malachite green oxalate, 10 mM sodium molybdate, 0.5% Triton X-100, 0.7 M HCl), which both quenched the reaction and provided the detection of P_i. The absorbance of each sample was measured at 680 nm after 10 min, and this was converted to $[P_i]$ from a P_i standard curve. Data was fitted to a single exponential plus steady-state curve (Eq. S2) using GraphPad Prism

Numerical Modeling. The stopped-flow light-scattering data shown in Fig. 4 were globally fitted to a system of simultaneous first-order differential equations corresponding to the reaction mechanism in Scheme 1, using the software DYNAFIT (29, 30). The data analyzed were obtained under pseudo first-order conditions, where the [Hsc70] is in significant excess over [clathrin]. Model discrimination analysis was performed using the second-order Akaike information criterion, AIC_c (23, 31). Nonsymmetrical confidence intervals for model parameters were estimated using the profile-t method (32, 33). Details of model selection are shown in the accompanying SI Text.

1. Grant BD, Donaldson JG (2009) Pathways and mechanisms of endocytic recycling. *Nat Rev Mol Cell Biol* 10:597–608.
2. Brodsky FM, Chen CY, Knuehl C, Towler MC, Wakeham DE (2001) Biological basket weaving: Formation and function of clathrin-coated vesicles. *Annu Rev Cell Dev Biol* 17:517–556.
3. Kirchhausen T (2000) Clathrin. *Annu Rev Biochem* 69:699–727.
4. Schmid SL (1997) Clathrin-coated vesicle formation and protein sorting: An integrated process. *Annu Rev Biochem* 66:511–548.
5. Pearse BM, Robinson MS (1990) Clathrin, adaptors, and sorting. *Annu Rev Cell Biol* 6:151–171.
6. Eisenberg E, Greene LE (2007) Multiple roles of auxilin and hsc70 in clathrin-mediated endocytosis. *Traffic* 8:640–646.
7. Holstein SE, Ungewickell H, Ungewickell E (1996) Mechanism of clathrin basket dissociation: Separate functions of protein domains of the DnaJ homologue auxilin. *J Cell Biol* 135:925–937.
8. Ungewickell E, Ungewickell H, Holstein SE (1997) Functional interaction of the auxilin J domain with the nucleotide- and substrate-binding modules of Hsc70. *J Biol Chem* 272:19594–19600.
9. Barouch W, Prasad K, Greene LE, Eisenberg E (1997) Auxilin-induced interaction of the molecular chaperone Hsc70 with clathrin baskets. *Biochemistry* 36:4303–4308.
10. Jiang RF, Greener T, Barouch W, Greene L, Eisenberg E (1997) Interaction of auxilin with the molecular chaperone, Hsc70. *J Biol Chem* 272:6141–6145.
11. Gao B, Greene L, Eisenberg E (1994) Characterization of nucleotide-free uncoating ATPase and its binding to ATP, ADP, and ATP analogues. *Biochemistry* 33:2048–2054.
12. Ha JH, McKay DB (1994) ATPase kinetics of recombinant bovine 70 kDa heat shock cognate protein and its amino-terminal ATPase domain. *Biochemistry* 33:14625–14635.
13. Greene LE, Eisenberg E (1990) Dissociation of clathrin from coated vesicles by the uncoating ATPase. *J Biol Chem* 265:6682–6687.
14. Schlossman DM, Schmid SL, Braell WA, Rothman JE (1984) An enzyme that removes clathrin coats: Purification of an uncoating ATPase. *J Cell Biol* 99:723–733.
15. Prasad K, Heuser J, Eisenberg E, Greene L (1994) Complex formation between clathrin and uncoating ATPase. *J Biol Chem* 269:6931–6939.
16. Ungewickell E, et al. (1995) Role of auxilin in uncoating clathrin-coated vesicles. *Nature* 378:632–635.
17. Xing Y, et al. (2010) Structure of clathrin coat with bound Hsc70 and auxilin: Mechanism of Hsc70-facilitated disassembly. *EMBO J* 29:655–665.
18. Fotin A, et al. (2004) Structure of an auxilin-bound clathrin coat and its implications for the mechanism of uncoating. *Nature* 432:649–653.
19. Barouch W, Prasad K, Greene LE, Eisenberg E (1994) ATPase activity associated with the uncoating of clathrin baskets by Hsp70. *J Biol Chem* 269:28563–28568.
20. Prasad K, Barouch W, Greene L, Eisenberg E (1993) A protein cofactor is required for uncoating of clathrin baskets by uncoating ATPase. *J Biol Chem* 268:23758–23761.
21. Jiang J, Prasad K, Lafer EM, Sousa R (2005) Structural basis of interdomain communication in the Hsc70 chaperone. *Mol Cell* 20:513–524.
22. Schuermann JP, et al. (2008) Structure of the Hsp110:Hsc70 nucleotide exchange machine. *Mol Cell* 31:232–243.
23. Myung JI, Pitt MA (2004) Model comparison methods. *Method Enzymol* 383:351–366.
24. Ma Y, et al. (2002) Identification of domain required for catalytic activity of auxilin in supporting clathrin uncoating by Hsc70. *J Biol Chem* 277:49267–49274.
25. Jiang R, Gao B, Prasad K, Greene LE, Eisenberg E (2000) Hsc70 chaperones clathrin and primes it to interact with vesicle membranes. *J Biol Chem* 275:8439–8447.
26. Ahle S, Ungewickell E (1990) Auxilin, a newly identified clathrin-associated protein in coated vesicles from bovine brain. *J Cell Biol* 111:19–29.
27. Rapoport I, Boll W, Yu A, Bocking T, Kirchhausen T (2008) A motif in the clathrin heavy chain required for the Hsc70/auxilin uncoating reaction. *Mol Biol Cell*.
28. Mayer MP, Bukau B (2005) Hsp70 chaperones: Cellular functions and molecular mechanism. *Cell Mol Life Sci* 62:670–684.
29. Kuzmic P (1996) Program DYNAFIT for the analysis of enzyme kinetic data: Application to HIV proteinase. *Anal Biochem* 237:260–273.
30. Kuzmic P (2009) DynaFit—A software package for enzymology. *Method Enzymol* 467:247–280.
31. Burnham KB, Anderson DR (2002) *Model Selection and Multimodel Inference: A Practical Information-Theoretic Approach* (Springer-Verlag, New York).
32. Bates DM, Watts DG (1988) *Nonlinear Regression Analysis and Its Applications* (Wiley, New York).
33. Brooks I, Watts DG, Soneson KK, Hensley P (1994) Determining confidence intervals for parameters derived from analysis of equilibrium analytical ultracentrifugation data. *Method Enzymol* 240:459–478.

Supporting Information

Rothnie et al. 10.1073/pnas.1018845108

SI Text

Early Events in Clathrin Cage Disassembly: A Mathematical Model for Clathrin Cage Disassembly. This section describes the statistical analysis of stopped-flow data shown in Fig. 4 of the main text.

The Van Slyke–Cullen mechanism for ATP association and hydrolysis. Kuzmic (1) recently demonstrated that, under certain experimental conditions, the proper mathematical model for the progress of an enzyme reaction is a system of simultaneous first-order ordinary differential equations (ODEs) corresponding the Van Slyke–Cullen catalytic mechanism (2). It was demonstrated that this particular system of equations is kinetically equivalent to a more extensive system of differential equations corresponding to the classic Michaelis–Menten catalytic mechanism (3). In particular, the apparent bimolecular association rate constant k_1^* in Scheme S2 is not only theoretically but also numerically equivalent to the specificity number, $k_{cat} = k_1 k_3 / (k_2 + k_3)$.

In preliminary kinetic analyses of the stopped-flow data shown in Fig. 4 of the main text, we have verified that both kinetic models (Michaelis–Menten and Van Slyke–Cullen), when embedded into an overall multistep mechanism for clathrin disassembly, fit Fig. 4 equally well. For this reason, in subsequent analyses of our stopped-flow data, each consecutive pair of Hsc70-ATP association/ATP → ADP hydrolysis reactions was modeled essentially a Van Slyke–Cullen module (Scheme S2).

Alternative kinetic mechanisms considered in this study. In Schemes S3–S7 below, the mechanisms are given mnemonic names where "A" represents Hsc70-ATP association and "H" represents ATP → ADP hydrolysis. Thus, for example, the designation AHAH represents a sequential mechanism, in which two molecules of ATP are consumed such that the second Hsc70-ATP molecule associates only after the first ATP molecule is already hydrolyzed. In contrast, the designation "AAAH" represents a concerted mechanism, in which three Hsc70-ATP molecules are first associated and, only then, all three ATP molecules are hydrolyzed at once.

The mechanisms in Schemes S3 and S4 differ only in that in AHAHAH* (Scheme S3) all microscopic rate constants can attain unique values, whereas in AHAHAH (Scheme S4) all association and ATP hydrolysis steps are governed by the same microscopic rate constant, k_a and k_r, respectively. The meaning of symbols "C", "T", and so on is identical in both schemes.

DynaFit input script for model discrimination. DynaFit (4, 5) is a software package that can automatically construct a mathematical model for any arbitrary molecular mechanism, as a system of simultaneous first-order ODEs, from symbolic input.

The following is a listing of a DynaFit input file ("script" file) that was used to fit the experimental data shown in Fig. 4A and discriminate between the mechanistic Schemes S3–S7.

```
                         [task]

                  task = fit
                  data = progress
                  model = AAAH ?

                  [mechanism]

        CA + T  —> CAT        :  ka
        CAT + T —> CATT       :  ka
        CATT + T—> CATTT      :  ka
        CATTT   —> CADDD      :  kr

        CADDD   —> Prods      :  kd

   [constants] ; units are "uM", "seconds"

              ka  = 1 ?
              kr  = 10 ?
              kd  = 0.1 ?

                 [responses]

          CA    = 11 ?
          CAT   = 14 ?
        CATT  = 1 * CAT
        CATTT = 1 * CAT
        CADDD = 1 * CAT

               [concentrations]

               CA = 0.09

                 [progress]

        directory   ./examples/gus_clathrin3/data
              extension   txt

   file HSC_0_5-EQS │ offset = 0 ? │ conc CA = 0.09 , T = 0.5 ?
```

```
file HSC_1-EQS   | offset = 0 ? | conc CA = 0.09 ?, T =  1.0
file HSC_2-EQS   | offset = 0 ? | conc CA = 0.09 ?, T =   2 ?
file HSC_4-EQS   | offset = 0 ? | conc CA = 0.09 ?, T =   4 ?

                    [output]

directory ./examples/gus_clathrin3/output/fit-041-gus

                   [settings]

                   {Filter}

                TimeMin = 0.1
                TimeMax = 12
           ReadEveryNthPoint = 30

                      ;
                   [task]

                 task = fit
               data = progress
               model = AHAHAH ?

                 [mechanism]

   CA + T  -> CAT        :  ka
   CAT     -> CAD + Pi   :  kr
   CAD + T -> CADT       :  ka
   CADT    -> CADD + Pi  :  kr
   CADD + T -> CADDT     :  ka
   CADDT   -> CADDD + Pi :  kr

   CADDD   -> Prods      :  kd

                 [responses]

                 CA    = 11 ?
                 CAT   = 14 ?
                CAD   = 1 * CAT
                CADT  = 1 * CAT
                CADD  = 1 * CAT
                CADDT = 1 * CAT
                CADDD = 1 * CAT

                      ;
                   [task]

                 task = fit
               data = progress
               model = AAHAH ?

                 [mechanism]

   CA + T  -> CAT        :  ka
   CAT + T -> CATT       :  ka
   CATT    -> CADD + Pi  :  kr
   CADD + T -> CADDT     :  ka
   CADDT   -> CADDD + Pi :  kr

   CADDD   -> Prods      :  kd

                 [responses]

                 CA    = 11 ?
                 CAT   = 14 ?
                CATT  = 1 * CAT
                CADD  = 1 * CAT
                CADDT = 1 * CAT
                CADDD = 1 * CAT

                      ;
                   [task]
```

```
                        task = fit
                       data = progress
                       model = AHAH ?

                       [mechanism]

          CA + T   —> CAT         :   ka
          CAT      —> CAD + Pi    :   kr
          CAD + T  —> CADT        :   ka
          CADT     —> CADD + Pi   :   kr
          CADD     —> Prods       :   kd

                       [responses]

            CA    = 11 ?
            CAT   = 14 ?
           CAD    = 1 * CAT
           CADT   = 1 * CAT
           CADD   = 1 * CAT


                            ;
                         [task]

                        task = fit
                       data = progress
                       model = AXBYCZ ?

                       [mechanism]

          CA + T   —> CAT          :   ka
          CAT      —> CAD + Pi     :   kx
          CAD + T  —> CADT         :   kb
          CADT     —> CADD + Pi    :   ky
          CADD + T —> CADDT        :   kc
          CADDT    —> CADDD + Pi   :   kz

          CADDD    —> Prods        :   kd

                       [responses]

            CA    = 7.16 ?
            CAT   = 8.77 ?
           CAD    = 1 * CAT
           CADT   = 1 * CAT
           CADD   = 1 * CAT
           CADDT  = 1 * CAT
           CADDD  = 1 * CAT

      [constants] ; units are "uM", "seconds"

              ka   = 0.69 ?
              kb   = 0.69 ?
              kc   = 0.69 ?
              kx   = 6.5 ?
              ky   = 6.5 ?
              kz   = 6.5 ?
              kd   = 0.38 ?
                 [end]
                    ;
```

Model discrimination analysis for Schemes S3–S7. Table S2 shows the results of the model discrimination analysis for Schemes S3–S7.

The "best" mechanistic model in terms of the residual sum of squares (RSS) was AHAHAH* (Scheme S3), in which three Hsc70-ATP molecules are associated in sequence, such that each consecutive association occurs only after the preceding ATP molecule is hydrolyzed. In this model, all three association rate constants and all three hydrolysis rate constants are allowed to attain unique values in the nonlinear regression.

However, despite the fact that the AHAHAH* model produced the lowest possible residual sum of squares, its Akaike weight (w in the right-most column) is zero, meaning that the

model is entirely implausible. This is because the "next best" model in terms of RSS (AHAHAH, Scheme S4) resulted in only 0.9% higher RSS value but—very importantly—it has four fewer adjustable model parameters (15 instead of 19) compared to AHAHAH*. The Akaike information criterion (AIC_c) appropriately penalizes fitting models containing large number of adjustable parameters. The AHAHAH three-step sequential kinetic model is associated with the highest Akaike weight ($w = 0.80$, nominally 80% probability that the AHAHAH model is true).

The next most plausible model is AAHAH, the three-step semiconcerted mechanism, which resulted in Akaike weight $w = 0.20$ (nominally 20% probability of being the true model).

Practical experience, as well as heuristic rules presented by others (6), suggest that a candidate regression model can be reliably dismissed only if the Akaike weight is lower than 0.05 or even 0.01. Therefore, we must conclude that it is virtually impossible to distinguish between the three-step semiconcerted mechanism (AAHAH, Scheme S7) and the most highly preferred, three-step sequential mechanism (AHAHAH, Scheme S4).

In contrast, we can say with very high degree of confidence that the two-step sequential mechanism (AHAH, Scheme S3) and the three-step concerted mechanism (AAAH, Scheme S4) can be reliably dismissed as not applicable. Not only is the residual sum of squares associated with these two mechanisms 20% higher, but, even more importantly, the ΔAIC_c criterion is higher than 20. Burnham and Anderson (6) state that candidate mathematical models associated with ΔAIC_c values higher than approximately 10 (and with Akaike weights very nearly approaching zero) indeed can be reliably dismissed.

SI Materials and Methods

Materials. We thank Jörg Höhfeld (Institute for Cell Biology, Rheinische Friedrich-Wilhelms-University Bonn, Germany) for the pVL1393-hsc70 plasmid. Spodoptera frugiperda (Sf9) cells and recombinant baculovirus expressing the full-length rat 70-kDa heat-shock cognate protein (Hsc70) were a kind gift from Yvonne Vallis and Harvey McMahon (Medical Research Council Laboratory of Molecular Biology, Cambridge, United Kingdom). The plasmid pGEX4T2-aux401-910 was a kind gift from Helen Kent (Medical Research Council Laboratory of Molecular Biology, Cambridge, United Kingdom). Fresh pig brains were obtained from an abattoir and frozen immediately before transportation. Hydroxyapatite Bio-Gel HT media and the DC Protein Assay Kit were from Biorad. Sephacryl S500 media, Superdex 200 media, Superdex 75 media, the GSTrapFF column, and thrombin protease were all obtained from GE Healthcare. Complete protease inhibitor cocktail tablets were from Roche Diagnostics. Chemically defined lipid concentrate was from Invitrogen. Isopropyl-b-D-thiogalactoside (IPTG) and aminoethylbenzenesulfonyl-fluoride (AEBSF) from Melford. ATP-agarose, TNM-FH insect cell media, ATP, ATPγS, AMPPNP, ADP, NADH, Phosphoenol-pyruvate, Pyruvate Kinase/Lactate Dehydrogenase mix, Malachite Green Oxalate, Sodium Molybdate, Triton X-100, and Ficoll PM70 were all obtained from Sigma Aldrich. Carbon film electron microscopy grids were from Agar Scientific.

Insect Cell Culture, Expression, and Purification of Hsc70. Full-length, rat Hsc70 was purified from Sf9 cells infected with a recombinant baculovirus carrying the plasmid pVL1393-hsc70 (7). Sf9 cells were maintained at $0.5-2.5 \times 10^6$ cells/mL in shaker cultures at 28 °C in TNM-FH media supplemented with 10% (vol/vol) fetal bovine serum, 1% (vol/vol) chemically defined lipids, 100 U/mL penicillin, and 100 mg/mL streptomycin. Hsc70 expressing baculovirus (1×10^8 pfu/mL) was amplified by infection of Sf9 cells (1×10^6 cells/mL) at a multiplicity of infection (MOI) of 0.2 for 5 d. Hsc70 expression in Sf9 cells was achieved by infection with the baculovirus at an MOI of 5 for 3 d. Cells were then harvested by centrifugation (7000 × g, 10 min) and frozen at −20 °C until required. Cells were thawed, resuspended in buffer 1 (20 mM Hepes pH7, 25 mM KCl, 3 mM MgCl$_2$) supplemented with a protease inhibitor cocktail tablet, and sonicated before centrifugation at 48,000 × g for 20 min. Hsc70 was purified from the soluble cell extract by a three-step process. Firstly, it was loaded on a hydroxyapatite biogel HT column, washed with buffer 1 supplemented with 20 mM K$_2$PO$_4$, and eluted with buffer 1 supplemented with 200 mM K$_2$PO$_4$. This was then loaded on to an ATP-agarose column, washed with buffer 1 supplemented with 1 M KCl, and eluted with buffer 1 supplemented with 3 mM

ATP and 0.1 mM AEBSF. A final purification step was carried out via a Superdex 75 gel filtration column, which also effectively removed excess ATP. The purified Hsc70 was concentrated and dialyzed into buffer 2 (40 mM Hepes pH7, 75 mM KCl, 4.5 mM Mg acetate). Extensive dialysis against activated charcoal was carried out at this stage to remove any remaining bound nucleotide. The concentration of Hsc70 was determined from A_{280} using an extinction coefficient of 3.3×10^4 M^{-1} cm^{-1} (ProtParam) and/or Biorad's DC protein assay kit. Hsc70 was aliquoted and stored at −70 °C for up to 1 y. An absorbance scan of the purified Hsc70 revealed that no detectable nucleotide was present. Full-length Hsc70 was chosen for these studies because it was more physiologically relevant. We experienced no issues with solubility, and this allowed us to be consistent with Schuermann et al., who also used light-scattering methods to investigate disassembly kinetics (8).

Expression and Purification of GST-auxilin$_{401-910}$. Residues 401–910 of bovine auxilin were expressed as a GST-fusion protein by transformation of *Escherichia coli* BL21 cells with the pGEX4T2-aux$_{401-910}$ plasmid. Overnight cultures (5 mL) were used to inoculate 1-L flasks of LB containing ampicillin and grown at 37 °C. Upon reaching A_{600} of 0.6, expression was induced by addition of 0.5 mM IPTG and incubated overnight. Cells were harvested by centrifugation (10,000 × g, 10 min) and frozen at −20 °C until needed. Cell pellets were thawed, resuspended in buffer 3 (20 mM Hepes pH7.2, 200 mM NaCl), supplemented with a protease inhibitor cocktail tablet, sonicated, and centrifuged (48,000 × g, 20 min). GST-auxilin$_{401-910}$ was affinity purified from the cell lysate by loading on a GSTrapFF column, washing thoroughly with buffer 3, and then eluting with buffer 3 supplemented with 10 mM glutathione (GSH). The purified GST-auxilin was dialyzed into buffer 2. The concentration of GST-auxilin$_{401-910}$ was determined from A_{280} using an extinction coefficient of 10.15×10^4 M^{-1} cm^{-1} (ProtParam) and/or Biorad's DC protein assay kit. GST-auxilin$_{401-910}$ was aliquoted, snap-frozen in liquid nitrogen, and stored at −70 °C for up to 6 mo; it is referred to elsewhere in this work simply as auxilin.

Purification of Clathrin from Pig Brain. Clathrin was purified from clathrin-coated vesicles that were extracted from pig brain. Approximately eight pig brains, which had been frozen in liquid N$_2$ shortly after harvesting, were homogenized in a blender with buffer 4 (25 mM Hepes pH7, 125 mM K acetate, 5 mM Mg acetate, 0.02% sodium azide) supplemented with protease inhibitor tablets. Following a low-speed spin to clarify this homogenate (12,000 × g, 30 min, 4 °C), it was subjected to ultracentrifugation at 140,000 × g, 45 min, 4 °C, to pellet lipid membrane components. The pellets were resuspended in approx. 50 mL of buffer 4 and homogenized. This was then mixed with an equal volume of 6.25% Ficoll/6.25% sucrose and spun at 44,000 × g, 20 min, 4 °C. This Ficoll/sucrose treatment causes clathrin-coated vesicles to stay in the supernatant. The coated vesicles can then be harvested from the supernatant by diluting out the Ficoll/sucrose and again submitting the sample to ultracentrifugation (140,000 × g, 1 h, 4 °C). The clathrin-coated vesicles were resuspended in a small volume of buffer 4 and homogenized, and a microfuge step removed small cytoskeletal contaminants. The protein coats were stripped off of the lipids by mixing the sample with an equal volume of 2× buffer 5 [1 M Tris, 1 mM EDTA, 0.1% (vol/vol) β-mercaptoethanol, 0.02% (wt/vol) sodium azide] and incubating for 1 h at 4 °C, followed by centrifugation to remove most of the lipids (135,000 × g, 20 min, 4 °C). Clathrin was purified from these "stripped, coated vesicles" firstly by loading on a Sephacryl S500 column equilibrated in buffer 5, which separated clathrin from remaining lipids and the various adaptor proteins present in coated vesicles. Clathrin was concentrated by ammonium sulphate precipitation, which also helped to remove contaminants,

and dialyzed before loading on a Superdex 200 column to clean it up finally. The pure clathrin was again concentrated by ammonium sulphate precipitation, before dialysis into buffer 6 [20 mM triethanolamine pH8, 1 mM EDTA, 0.1% (vol/vol) β -mercaptoethanol, 0.02% (wt/vol) sodium azide]. Clathrin cages were formed in vitro by dialyzing the sample into buffer 7 [100 mM MES pH6.5, 15 mM $MgCl_2$, 0.2 mM EGTA, 0.02% (wt/vol) sodium azide], and harvested by centrifugation ($135,000 \times g$, 20 min, 4 °C). Cages were resuspended in approximately 200 μL of buffer 7 and stored at 4 °C for up to 1 mo. The concentration of deploymerized clathrin was determined from the A_{280} using an extinction coefficient of 230,900 $M^{-1} cm^{-1}$.

Steady-State ATPase Assay. The steady-state ATPase activity of Hsc70, both alone and when stimulated by auxilin, was monitored using an enzyme coupled assay for ADP release, as described previously (9). Briefly, the coupling enzymes (pyruvate kinase 20 U/mL and lactate dehydrogenase 25 U/mL), phosphoenol pyruvate (2 mM), ATP (500 μM), and NADH (0.3 mM) were incubated at 25 °C in the presence of auxilin (0–16 μM) in buffer 2, and absorbance was monitored at 340 nm. The assay was initiated by addition of Hsc70 (4 μM). As ADP was produced, the amount of NADH decreased and thus the absorbance at 340 nm decreased. From the extinction coefficient for NADH and using Beer's Law, the rate of decrease in A_{340} could be converted to a rate of ATP hydrolysis.

To examine the stimulatory effect of clathrin cages on the ATPase activity of Hsc70, the assay buffer was decreased to pH6, to prevent disassembly of the clathrin cages (10). The concentration of auxilin was kept constant at 4 μM, and the concentration of Hsc70 was decreased to 2 μM, whereas the concentration of clathrin was varied from 0–2.7 μM triskelia.

Isothermal Titration Calorimetry (ITC). Binding of Hsc70 to ATP, ADP, or auxilin was measured by ITC, using a VP-ITC (MicroCal), to give equilibrium binding parameters. ATP in the syringe (50 μM) was added to Hsc70 in the cell (5 μM in buffer 2) in a series of 25 injections with 300 s between each injection, at a

temperature of 10 °C to prevent any significant amount of ATP hydrolysis. The heat of dilution of ATP into buffer was subtracted from the results prior to analysis. The titration curves were analyzed using Origin software as provided by the manufacturer, yielding values for the stoichiometry and the affinity of the interaction. The interaction of Hsc70 with ADP was carried out essentially the same way, but at 20 °C to get a larger signal, because hydrolysis was not an issue. The interaction of Hsc70 with auxilin was also similar, except the auxilin was in the cell and Hsc70 in the syringe, and ATP was present in both chambers.

Stopped-Flow Perpendicular Light-Scattering Mixing-Order Experiments. The effect of preincubation on ice for 30 min of reaction components was monitored using stopped-flow perpendicular light-scattering experiments. These experiments were performed as described in the *Materials and Methods* section of the main text, with the specific conditions given in Table S3. Syringes were always mixed at ratio 2:1:1, syringe 1:syringe 2:syringe 3. Clathrin concentrations are given in terms of triskelia.

Equations.

$$Y = A - B \frac{[S]}{K + [S]}, \qquad [\text{S1}]$$

where Y is quantity such as $t_{1/2}$ or amplitude (Fig. 2 of main text), A is an empirical constant corresponding to offset of the y axis, B is an empirical constant corresponding to amplitude, K is an empirical constant corresponding to half-maximum effect, and $[S]$ is Hsc70 concentration.

$$A = A_0[1 - \exp(-kt)] + vt, \qquad [\text{S2}]$$

where A is observed signal, A_0 is exponential amplitude, k is first-order rate constant, t is time, and v is constant steady-state rate.

1. Kuzmic, P. (2009a) Application of the Van Slyke-Cullen irreversible mechanism in the analysis of enzymatic progress curves. *Anal. Biochem.*, **394**, 287–289.
2. van Slyke, D.D. and Cullen, G.E. (1914) The mode of action of urease and of enzymes in general. *J. Biol. Chem.*, **19**, 141–180.
3. Michaelis, L. and Menten, M.L. (1913) Die Kinetik der Invertinwirkung. *Biochem. Z.*, **49**, 333–369.
4. Kuzmic, P. (1996) Program DYNAFIT for the analysis of enzyme kinetic data: Application to HIV proteinase. *Anal. Biochem.*, **237**, 260–273.
5. Kuzmic, P. (2009b) DynaFit—A software package for enzymology. *Meth. Enzymol.*, **467**, 247–280.
6. Burnham, K.B. and Anderson, D.R. (2002) *Model Selection and Multimodel Inference: A Practical Information-Theoretic Approach.* Springer-Verlag, New York.
7. Hohfeld, J. and Jentsch, S. (1997) GrpE-like regulation of the hsc70 chaperone by the antiapoptotic protein BAG-1. *EMBO J.*, **16**, 6209–6216.
8. Schuermann JP, Jiang J, Cuellar J, Llorca O, Wang L et al. (2008) Structure of the Hsp110:Hsc70 nucleotide exchange machine *Moll. Cell.* **31**, 232–243.
9. Kreuzer, K.N. and Jongeneel, C.V. (1983) Escherichia coli phage T4 topoisomerase. *Meth. Enzymol.*, **100**, 144–160.
10. Barouch, W., Prasad, K., Greene, L.E. and Eisenberg, E. (1997) Auxilin-induced interaction of the molecular chaperone Hsc70 with clathrin baskets. *Biochemistry*, **36**, 4303–4308.
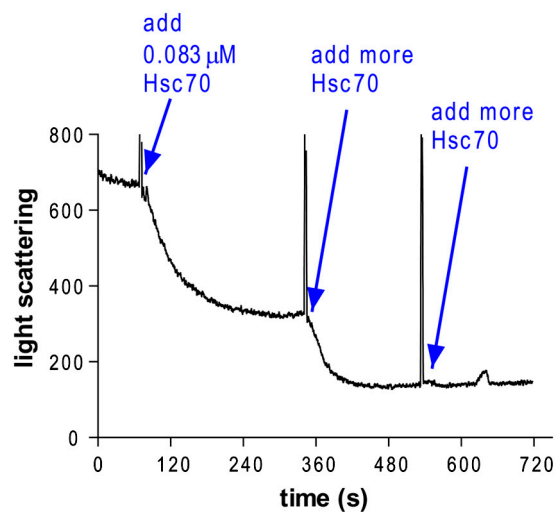
Fig. S1. Clathrin cage disassembly does not proceed to completion when the concentration of Hsc70 is limiting. Light-scattering curve obtained using clathrin cages (0.09 μM triskelia), 0.1 μM auxilin, and 500 μM nucleotide and initiated by addition of 0.083 μM Hsc70. Cage disassembly reaches a plateau with some cages remaining under such conditions of limiting Hsc70. However, subsequent addition of excess Hsc70 does allow disassembly to proceed to completion. Further addition of Hsc70 has no effect once disassembly of all cages has occurred.
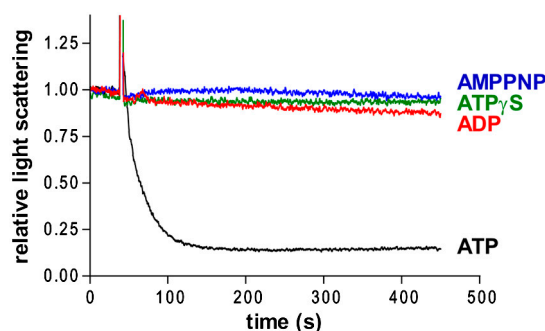
Fig. S2. Nonhydrolyzable nucleotides do not support clathrin cage disassembly. Light-scattering curves obtained using clathrin cages (0.09 μM triskelia), 0.1 μM auxilin, 2 μM Hsc70, and 500 μM nucleotide, either ATP (black), ADP (red), ATPγS (blue), or AMPPNP (green). The AMPPNP was pretreated with hexokinase and glucose prior to use to remove contaminating ATP.
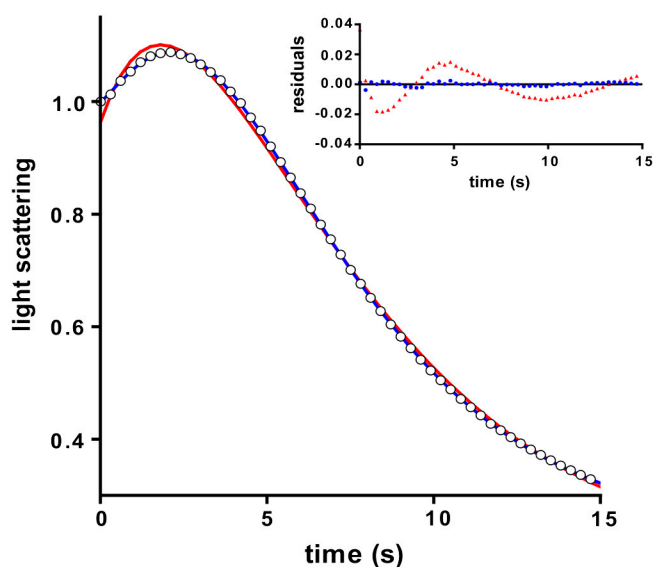
Fig. S3. The stopped-flow clathrin disassembly curves are fitted well by a triple exponential. A clathrin disassembly curve ([Hsc70] = 2 μM), fitted with either a double exponential (red) or a triple exponential (blue). *Inset* shows the residuals to the curve fits. There is a clear improvement in the fit when the triple exponential is used.
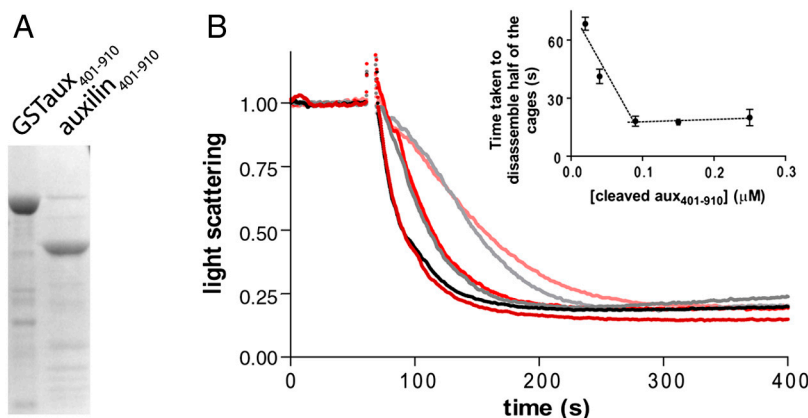
Fig. S4. The GST tag has no effect on the function or optimal stoichiometry of auxilin in clathrin disassembly assays. (*A*). SDS-PAGE showing purified GST-auxilin$_{401-910}$ and following cleavage with thrombin (10 U thrombin/mg GST-auxilin, 1.5 h, 25 °C) and removal of GST via binding to GSH-sepharose beads. (*B*) Representative clathrin cage disassembly curves (0.09 μM triskelia, 2 μM Hsc70, 500 μM ATP) comparing GST-auxilin (black, dark gray, and light gray) with cleaved auxilin (dark red, red, and pink), at concentrations of 0.1 μM (black and dark red), 0.04 μM (dark gray and red) or 0.02 μM (light gray and pink). (*Inset*) Average times taken for disassembly of half of the clathrin cages using various concentrations of cleaved auxilin. Data are mean ± SEM, *n* = 3.
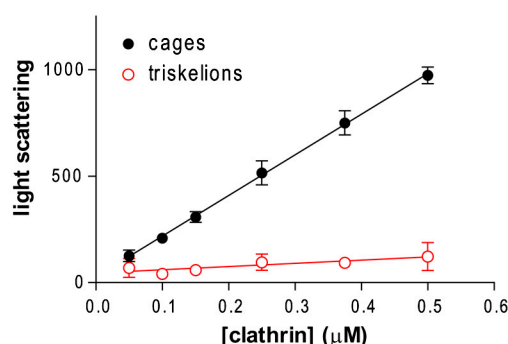
Fig. S5. The scattering signal obtained from clathrin cages or clathrin triskelia is linearly dependent on the clathrin concentration. Right-angle light scattering at 390 nm obtained from various concentrations of clathrin cages (black, closed circles) and free triskelions (red, open circles).
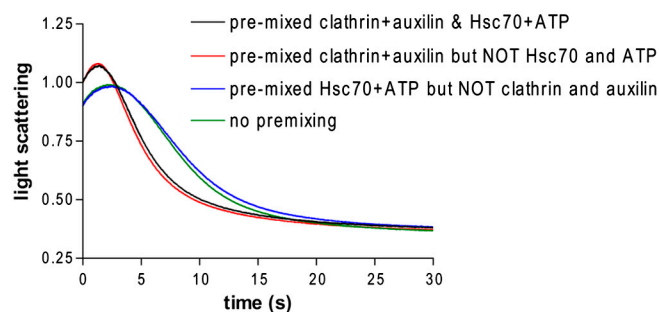
**Fig. S6.** The binding of ATP to Hsc70 is very fast and does not limit the rate of clathrin cage disassembly. Stopped-flow light-scattering curves obtained using clathrin cages (0.09 μM triskelia), 0.1 μM auxilin, 2 μM Hsc70, and 500 μM ATP (final concentrations after mixing). The effect on the rate of cage disassembly of premixing components on ice for 30 min prior to initiating disassembly was examined. Full experimental details are given in the supplementary text. Experiment 1 (black line), preincubated clathrin and auxilin mixed with preincubated Hsc70 and ATP; experiment 2 (red line), preincubated clathrin and auxilin mixed separately with Hsc70 and ATP; experiment 3 (blue line), preincubated Hsc70 and ATP mixed separately with clathrin and auxilin; experiment 4 (green line), all four components mixed with no preincubation step.

Table S1. Parameters for the interaction of Hsc70 with nucleotide and auxilin

	K_d, μM	Stoichiometry		k (s^{-1})	Fold stimulation
ATP binding*	0.065 ± 0.010	0.62 ± 0.09	ATP hydrolysis[†]	0.0011 ± 0.0002	1.0
ADP binding*	0.16 ± 0.04	0.57 ± 0.13	+ auxilin[†]	—	12.4 ± 1.4
Auxilin binding* (in the presence of ATP)	0.20 ± 0.04	0.80 ± 0.06	+ clathrin only[†]	—	1.2 ± 0.1
			+ auxilin + clathrin[†]	—	51.3 ± 2.8

*Binding parameters determined by isothermal titration calorimetry.
[†]ATP hydrolysis rates determined using a pyruvate kinase/lactate dehydrogenase coupled assay for ADP release. Data are mean ± SD.

Table S2. Model discrimination analysis for Schemes S3–S7

Model	Scheme	P	RSS	ΔAIC_c	w
AHAHAH*	S3	19	1.000	8.7	0.000
AHAHAH	S4	15	1.009	0.0	0.796
AHAH	S5	15	1.195	27.8	0.000
AAAH	S6	15	1.165	23.6	0.000
AAHAH	S7	15	1.026	2.8	0.194

P is the number of adjustable model parameters; RSS is the relative sum of the squares, ΔAIC_c is the increase in the second-order Akaike information criterion relative to the best model ($\Delta AIC_c = 0$), and w indicates the Akaike weight such that $0.10 = 10\%$ probability that the given mechanistic model is true.

Table S3. Stopped-flow perpendicular light-scattering mixing-order experiments

Experiment	Syringe 1	Syringe 2	Syringe 3
1. Premixing clathrin with auxilin AND Hsc70 with ATP	clathrin (0.18 μM) and auxilin (0.2 μM) preincubated together on ice for 30 min	Hsc70 (8 μM) and ATP (2 mM) preincubated together on ice for 30 min	buffer only
2. Premixing clathrin with auxilin, but NOT Hsc70 with ATP	clathrin (0.18 μM) and auxilin (0.2 μM) preincubated together on ice for 30 min	Hsc70 (8 μM)	ATP (2 mM)
3. Premixing Hsc70 with ATP, but NOT clathrin with auxilin	clathrin (0.18 μM)	Hsc70 (8 μM) and ATP (2 mM) preincubated together on ice for 30 min	auxilin (0.4 μM)
4. No premixing	clathrin (0.18 μM)	Hsc70 (8 μM)	auxilin (0.4 μM) ATP (2 mM)

$$E + S \underset{}{\overset{k_1}{\rightleftharpoons}} E.S \overset{k_3}{\longrightarrow} E$$

Scheme S1. Michaelis–Menten mechanism for enzyme catalysis.

$$E + S \overset{k_1^*}{\longrightarrow} E.S \overset{k_3}{\longrightarrow} E + P$$

Scheme S2. Van Slyke–Cullen mechanism for enzyme catalysis.

$$C \xrightarrow[k_a]{+T} CT \xrightarrow{k_r} CD \xrightarrow[k_a]{+T} CDT \xrightarrow{k_r} CDD \xrightarrow[k_a]{+T} CDDT \xrightarrow{k_r} CDDD \xrightarrow{k_d} P$$
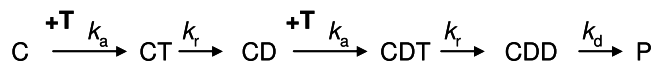
C = clathrin•auxilin
T = Hsc70•ATP
D = Hsc70•ADP
P = products.

Scheme S3. Mechanism AHAHAH* (three-step sequential, unique rate constants).

$$C \xrightarrow[k_a]{+T} CT \xrightarrow{k_r} CD \xrightarrow[k_a]{+T} CDT \xrightarrow{k_r} CDD \xrightarrow[k_a]{+T} CDDT \xrightarrow{k_r} CDDD \xrightarrow{k_d} P$$

Scheme S4. Mechanism AHAHAH (three-step sequential, identical rate constants).

$$C \xrightarrow[k_a]{+T} CT \xrightarrow{k_r} CD \xrightarrow[k_a]{+T} CDT \xrightarrow{k_r} CDD \xrightarrow{k_d} P$$

Scheme S5. Mechanism AHAH (two-step sequential). This mechanism differs from "AHAHAH" (Scheme S4) above only in that two molecules of ATP are consumed instead of three.

$$C \xrightarrow[k_a]{+T} CT \xrightarrow[k_a]{+T} CTT \xrightarrow[k_a]{+T} CTTT \xrightarrow{k_r} CDDD \xrightarrow{k_d} P$$
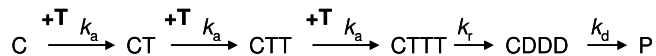
Scheme S6. Mechanism AAAH (three-step concerted). Here, all three ATP molecules are first associated, and they hydrolyzed at once.

$$C \xrightarrow[k_a]{+T} CT \xrightarrow[k_a]{+T} CTT \xrightarrow{k_r} CDD \xrightarrow[k_a]{+T} CDDT \xrightarrow{k_r} CDDD \xrightarrow{k_d} P$$

Scheme S7. Mechanism AAHAH (Three-step semiconcerted). Two molecules of ATP are associated, and both are then hydrolyzed at once. After this, the third ATP molecule is associated and hydrolyzed.